Hindawi
Advances in Materials Science and Engineering
Volume 2019, Article ID 9071034, 15 pages
https://doi.org/10.1155/2019/9071034

Research Article

Hardening Concrete Exposed to Realistic Curing Temperature Regimes and Restraint Conditions: Advanced Testing and Design Methodology

Anja Estensen Klausen,[1] **Terje Kanstad**,[1] **and Øyvind Bjøntegaard**[2]

[1]*Norwegian University of Science and Technology (NTNU), Department of Structural Engineering, Richard Birkelandsvei 1a, 7491 Trondheim, Norway*
[2]*Norwegian Public Roads Administration, Road Directorate, Tunnel and Concrete Section, Abels Gate 5, 7030 Trondheim, Norway*

Correspondence should be addressed to Anja Estensen Klausen; anja.klausen@ntnu.no

Received 3 October 2019; Revised 21 November 2019; Accepted 27 November 2019; Published 14 December 2019

Academic Editor: Aniello Riccio

Early age cracking (EAC) is a well-known problem area when it comes to concrete structures. The driving forces behind EAC are thermal dilation and autogenous deformation, but EAC is also strongly dependent on material and geometrical properties such as hydration heat development, tensile strength, E-modulus, creep, cross-sectional dimensions, and degree of restraint. The current document contains a description of the EAC design methodology that is currently being implemented in Norway. The basis of the methodology is to define and describe the material properties of a given concrete through laboratory testing and succeeding model fitting. The obtained material parameters are then evaluated and calibrated by comparing (1) stress development measured in a Temperature-Stress Testing Machine with (2) stress development calculated by using the obtained material properties and various multiphysical EAC calculation approaches. Special consideration is given to the effect of realistic curing temperature regimes on the various material properties and consequently on the EAC.

1. Introduction

Early age cracking (EAC) can prove a challenge when it comes to concrete structures. The major concern when it comes to EAC is "through-cracking," which may go through the whole thickness of the concrete member and further lead to functionality, durability, and esthetical problems. EAC is induced by restrained volume changes occurring in the hardening phase, where the driving forces are thermal dilation (TD) and autogenous deformation (AD). EAC is also strongly dependent on material and geometrical properties such as hydration heat development, coefficient of thermal expansion (CTE), tensile strength, E-modulus, creep, cross-sectional dimensions, and degree of restraint. Early age crack assessment constitutes a combination of structural analysis and materials science; the volume changes of concrete and the associated cracking risk can be predicted by the use of calculation methods to assess the early age structural behaviour of the concrete, where the above-described material and geometrical properties are important input parameters. On the basis of such EAC calculations and in combination with good knowledge of the material properties of relevant concretes, proper choice of concrete type, mineral additives, and execution methods on site can be taken to minimize or even avoid cracking.

Various approaches at EAC calculations can be found in the literature. Examples of guidelines and prevailing regulations regarding cracking and design in the serviceability limit state (SLS) with respect to early age volume changes are Eurocode 2, CIRIA C766, Model Code 2010, CEOS.fr, NS3473, JCI Guideline, and BAW Guideline [1–7]. While some EAC design approaches merely are an estimation of whether the concrete will crack or not, other approaches also provide calculation methods that predict the size of the

subsequent occurring crack widths. Common for all EAC calculation methods is that the accuracy of the outcome is very dependent on the quality and correctness of the material parameters used as input. An accurate characterization of the development of relevant material properties is therefore of great importance when it comes to the EAC design.

Material properties of concrete can be determined by laboratory experiments or more commonly by models found in guidelines and codes. The latter will automatically cause a degree of uncertainty to the EAC calculation results as several of the required material input parameters are complex and dependent on mix design, w/c-ratio, time, degree of hydration, curing temperature, etc. For instance, a weakness in most concrete material property mappings is that they are based on 20°C isothermal conditions and do not account for a realistic temperature curing regime [8]. This contradicts the fact that several studies state that a realistic curing regime may affect material properties such as AD, CTE, tensile strength, E-modulus, and compressive strength of concrete in a way that cannot be accounted for by the maturity principle [9–16].

Although not very common, early age stress development can be measured by specially designed experimental equipment. In 1969, the Cracking Frame was developed in München, Germany [17]. The Cracking Frame measured the stress response of concrete at early ages to changing temperatures in a concrete specimen with high, but unknown, restraint. In 1984, Springenschmid et al. developed the improved Temperature-Stress Testing Machine (TSTM) that was temperature and deformation controlled giving 100% restraint. Today, several different TSTM variants and other similar devices measuring stress development in hardening concrete are found around the world [12, 18–25]. The TSTM at NTNU was built in 1995, and in 2012 it was reconstructed with a new measuring set-up and new software that, among other factors enabled the unique opportunity to define and simulate a predefined degree of restraint during testing [15, 26]. The TSTM at NTNU is temperature controlled, and it is constructed to measure the one-dimensional stress generation in a sealed concrete specimen through the hardening phase at a chosen degree of restraint. By applying a representative degree of restraint and temperature history, the TSTM is able to directly simulate the stress development over time for a given section of a concrete structure. In combination with multiphysical EAC analyses and "back-calculations," the TSTM thus provides a unique opportunity to bridge the gap between laboratory experiments and actual behaviour at the construction site.

Research in the EAC field has expanded strongly internationally since the early 90s with the RILEM Munchen conference as a starting point [27]. This has resulted in several major conferences devoted directly to the topic or as special sessions at larger meetings [28–34]. In addition, large numbers of papers have been published in regular journals. Since the RILEM Munchen conference in 1994, the concrete group at NTNU has been strongly involved in the EAC field both on the materials and the experimental and computational aspects. The work has taken place both within EU and national projects involving industrial, institutional, and university participants. The outcome has been numerous publications, participations at international conferences, and workshops, as well as several Ph.D. theses [12, 15, 35–38].

Despite the above-described research in the field, dedicated EAC calculations have traditionally not been commonly included in structural design in Norway. Instead, requirements regarding maximum temperature increase and temperature gradients over the concrete cross section have been decisive [39]. Over the last decade, however, the focus on the EAC design has enhanced due to an increasing awareness in the industry, as well as a more frequently seen option to avoid temperature requirements by performing dedicated EAC calculations. In view of this, the currently presented material property characterization and EAC design approach has been established and developed within the research projects COIN [40] and DACS [41] over the recent years. The methodology aims to be pragmatic in the way that it includes high activity in the laboratory, and it is based on a close collaboration between research and industry in Norway. The overall aim has been to make the method accurate and advanced, but still practical and easy applicable for contractors and structural designers. The basis of the methodology is to define and describe the material properties of a given concrete through extensive laboratory testing and succeeding model fitting. The obtained material parameters are further evaluated and calibrated by comparing (1) stress development measured in the TSTM with (2) stress development calculated by multiphysical EAC calculation approaches using the obtained material properties. In the current study, special consideration has been given to the effect of a realistic temperature curing regime on the various material properties and consequently on the EAC risk.

The main objectives of the current work have been to develop and improve the above-described EAC design methodology and the corresponding concrete property characterization, including laboratory test methods. The laboratory work includes determination of decisive parameters for early age crack assessment, a parameter study on the fly ash content to show the relevance of the method, as well as several tests in the TSTM that form the basis of the work. An overall aim has been to make the EAC design methodology and the obtained data available for the Norwegian concrete industry. The need for a reliable and effective concrete property characterization and EAC design methodology is also rooted in the environmental aspect. In the years to come, concrete will change due to its current contribution to CO_2 emissions and its use of natural resources. The industry needs to be prepared for property characterization and EAC design of the upcoming next generation of concretes with low-CO_2 cements and recycled aggregate [42].

2. Experimental Equipment

The experimental equipment used in the current study is described as follows.

The hydration heat evolution of the concretes was measured by semiadiabatic calorimeter tests. 15 litre samples

of concrete were cast into plywood boxes insulated by 100 mm Styrofoam on all sides. During testing, the box was stored in air at 38°C while the air and concrete temperature was measured continuously for 5 days. The measured temperature development was converted to isothermal heat development as a function of maturity. The heat loss to the environment was calculated by assuming that the heat flow out of the box was proportional to the temperature difference between the concrete and the environment. The method is commonly used in Norway and described in NS 3657:1993 [43].

The compressive strengths of the investigated concretes were determined on 100 mm cubes, which is the standard specimen for compressive strength testing in Norway. The tests were performed in accordance with NS-EN 12390-3:2009.

The tensile strength and the tensile E-modulus were determined by uniaxial strength tests in an INSTRON 5985 electromechanical testing system [44], which has been the standard method for uniaxial tensile strength determination at SINTEF/NTNU in Norway for several years [45]. At each end of a $100 \times 100 \times 600$ mm vertically oriented specimen, tensile loading was applied by specially designed grips designed to ensure a uniform stress distribution. The tensile stress development was measured directly from the centre of the loading axis by a load cell system, up until the specimen developed failure in tension. During testing, two displacement transducers installed on opposite sides of the specimen measure the deformation over the 100 mm midsection. The strain rate during testing was approximately 100×10^{-6} per min. The load-deformation curve obtained during the tensile strength test was also used to calculate the tensile E-modulus. The tensile E-modulus was defined as the stress/strain-ratio between 10% and 40% of the failure load.

The stress development in the hardening phase was measured by the Temperature-Stress Testing Machine (TSTM) at NTNU. The TSTM system comprises a dilation rig and a TSTM, both connected to a temperature-control system (Julabo FP45), which provides an accurate control of the concrete temperature during testing.

The dilation rig is the "dummy" rig following the TSTM (Figure 1). It measures the free deformation, i.e., TD and AD, of a $100 \times 100 \times 500$ mm horizontally oriented concrete specimen. The dilation rig formwork is made of 5 mm thick copper plates surrounded by 5 mm copper pipes with circulating water connected to the temperature-control unit. The formwork and the copper pipes are covered with insulation. Movable end plates made of polystyrene and steel, respectively, are placed at each short end of the formwork, allowing the end plates and hence the concrete specimen to move freely during the experiment. Measuring bolts made of invar steel are cast directly into each short end of the concrete specimen. After casting, an inductive displacement transducer (LVDT) is mounted at each short end, providing a free connection between measuring bolts and LVDTs. The temperature-induced length change of the measuring bolts is calculated and compensated for in every experiment. Temperature measurements are started immediately after casting, while length change measurements are initiated after approximately 2 hours, depending on the concrete and its early stiffening characteristics. During testing, the concrete specimen is carefully sealed with plastic and aluminum foil.

The TSTM measures the stress development in the hardening phase at a given degree of restraint, R. The TSTM consists of an outer steel frame that, nearly frictionless, supports two movable crossheads and a movable midsection (Figures 1 and 2). Together, the two crossheads and the midsection constitute a formwork into which the horizontally oriented concrete specimen is cast. The TSTM formwork is composed in the same way as the dilation rig formwork, with 5 mm copper plates surrounded by 5 mm copper tubes (containing circulating temperature-controlled water) covered by insulation. The crossheads and the top covers are also temperature controlled, providing a uniform temperature history in the whole concrete specimen during testing. The TSTM concrete specimen is shaped as a "dog bone." The central 700 mm of the midsection, the measuring length, has a rectangular cross section with dimensions 88 mm (width) × 100 mm (height). Outside the measuring length, the width of the concrete cross section increases linearly on both sides until it reaches 100 mm at the crossheads. The cross-sectional width continues to increase gradually up to 225 mm within the crosshead, providing restraint for the concrete specimen. Prior to casting, two measuring bolts are installed in the TSTM midsection with a distance of 700 mm, defining the measuring length. The measuring bolts go through the temperature-controlled mould and are embedded in the concrete during casting. The concrete specimen deformation is measured as the length change between the two measuring bolts by two inductive displacement transducers (LVDTs), one on each side of the concrete specimen (see Figure 1). A load cell is mounted to the right crosshead, Figure 2, measuring the restraining force transferred through the concrete cross section during testing. During testing, the concrete specimen is carefully sealed with plastic and aluminum foil.

The software is connected to the LVDTs and the load cell, as well as to a high-precision screw moving the left crosshead (Figure 2). The magnitude of the crosshead movement induced by the software is decided by (1) the length change in the concrete measured by the LVDTs, (2) the load measured by the load cell, and (3) the user defined parameters in the software. The TSTM is by this both deformation controlled and load controlled. In addition, the new software allows the user to choose a desired degree of restraint in the range between 0 and 100%, where the degree of restraint is defined as the ratio between restrained and total deformation in the TSTM tests times 100%. For TSTM tests with a realistic temperature curing regime, R is normally set to 50%, which represents typical restraint conditions for a wall on a slab [47]. A degree of restraint of 50% provides a longer measurement period before the specimen develops failure in tension and thus provides more data than if the specimen was to be fully restrained.

The TSTM system has several areas of application. Subsequent to a restrained stress test, the coefficient of thermal expansion (CTE) can be found by applying a series of temperature steps of ±3°C around an initial temperature of 20°C to the TSTM system. In addition, results from

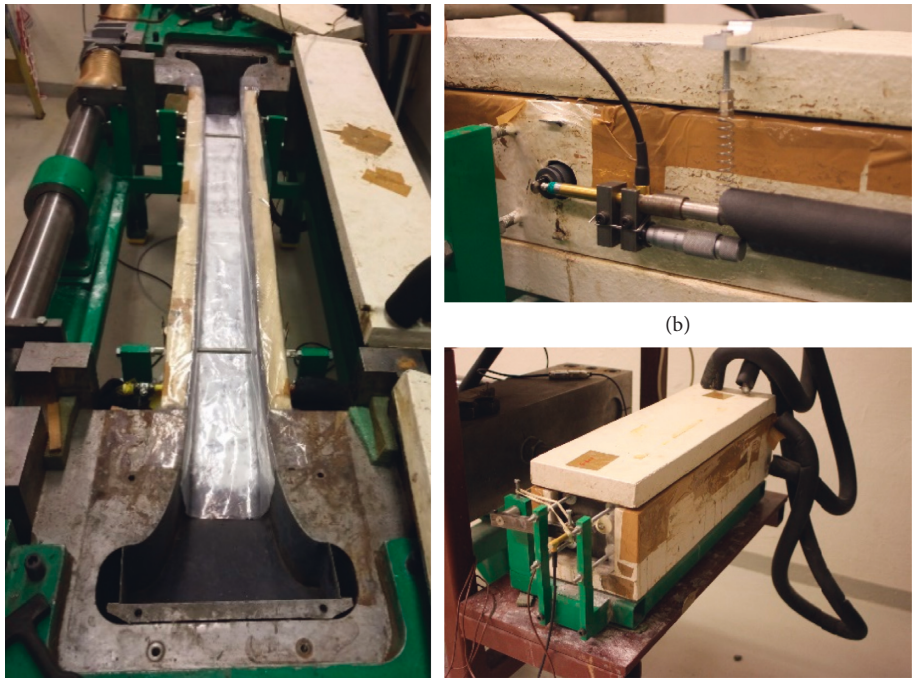

(a) (b) (c)

Figure 1: The TSTM system: the dog-bone form in the TSTM (a), the TSTM LVDT set-up (b), and the dilation rig (c).

restrained stress tests in the TSTM can be used to deduce the incremental E-modulus development over time as well as the starting time for stress development t_0 [46]. The TSTM can also be used for other experimental purposes than the previously described restrained stress measurements. Creep and relaxation tests as well as determination of restraint stresses due to drying shrinkage can be performed in the TSTM [38, 46, 48]. A detailed description of the TSTM system and its possibilities are given in [15].

It should be noticed that in the current study, the concrete specimens have been thoroughly sealed and it was therefore decided to neglect drying shrinkage. For massive concrete structures, and in a short-term perspective, drying shrinkage will be small and may generally be ignored.

3. Concrete Mix Design and Test Program

The current study includes four concretes: one reference concrete without fly ash (ANL ref.) and three concretes with a varying amount of fly ash (ANL FA17, ANL FA33, and ANL FA45). The concrete composition, as well as total fly ash content, is given in Table 1. The reference concrete, ANL ref., contains no fly ash, and it is made with Portland cement CEM I "Norcem Anlegg" [49]. The fly ash concretes, on the other hand, are made with Portland-fly ash cement CEM II/A-V "Norcem Anlegg FA," where 17% fly ash is interground with the clinker. All concretes were made with a water-to-binder ratio of 0.4 and a cement paste volume of 292 l/m^3. The fly ash content was increased by replacing cement with fly ash 1 : 1 by weight, while keeping the water-to-binder ratio and the cement paste volume constant. The fly ash content is given as a percentage of the total amount of cement + fly ash. A detailed cement composition can be found in [15].

The currently described methodology for the EAC design is the result of a close collaboration between research and industry in Norway. Consequently, the investigated concretes and fly ash contents were chosen based on common practice in the Norwegian concrete industry. The exception was the fly ash content of 45%, which was included in order to "challenge" the national regulations. The Norwegian Standard allows up to 35% fly ash, while the NPRA (Norwegian Public Roads Administration) allows up to 40% fly ash. Silica fume was added to the mix as it is an absolute requirement for all concrete used for infrastructural facilities in Norway [39].

Table 2 presents the experimental programme carried out in the current study. The programme includes hydration heat evolution, development of compressive strength, direct uniaxial tensile strength, and tensile E-modulus, as well as free deformation and restrained stress tests in the TSTM.

The current study focuses on early age cracking, where the E-modulus in tension is a main material property. In addition, the comparable incremental E-modulus development in the TSTM is mainly based on tensile load application. Due to this, the current article reports tensile E-modulus only. Corresponding compressive E-moduli for the investigated concretes are reported and compared with the currently presented tensile E-moduli in [15].

The TSTM tests were carried out under semiadiabatic conditions, i.e., each concrete was subjected to its own semiadiabatic temperature history representing a section of an 800 mm thick wall subjected to Norwegian summer or winter conditions. ANL FA17 and ANL FA45 were also

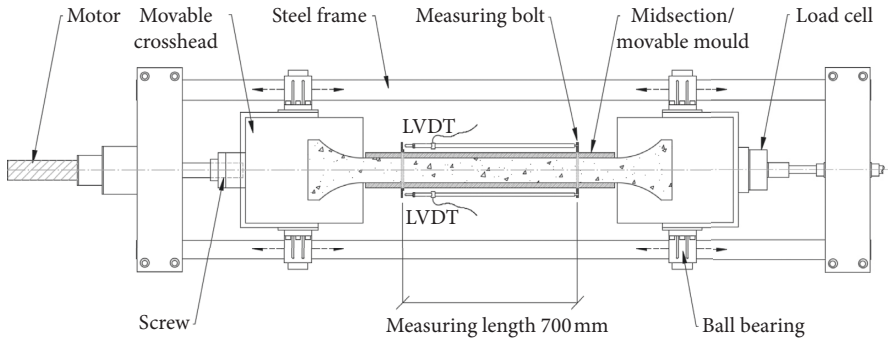

Figure 2: Sketch of the TSTM, after [46].

Table 1: Concrete mix design.

	ANL ref.	ANL FA17	ANL FA33	ANL FA45
Cement (kg/m^3)	372.3	365.3	284.3	229.8
FA_{cem} (FA included in the cement) (kg/m^3)	0.0	60.6	47.2	38.1
FA_{added} (additional FA added) (kg/m^3)	0.0	0.0	71.1	118.5
Silica fume (kg/m^3)	18.6	18.3	17.6	17.4
Free water (kg/m^3)	163.8	160.7	156.2	153.3
Sand 0–8 (kg/m^3)	1216.3	1216.3	1216.3	1216.3
Gravel 8–16 (kg/m^3)	614.1	614.1	614.1	614.1
Plasticizer (kg/m^3)	2.05	2.01	1.56	1.56
Assumed air content (%)	2.0	2.0	2.0	2.0
Theoretically density (kg/m^3)	2400	2390	2370	2360
Total FA content, FA/(cem + FA)	0%	25%	33%	45%
Silica fume content, silica/(cem + FA)	5%	5%	5%	5%

tested with temperature regimes representing Norwegian winter conditions. Norwegian summer conditions imply a fresh concrete temperature of 20°C and an ambient temperature of 20°C, while Norwegian winter conditions are represented by a fresh concrete temperature of 10°C and an ambient temperature of 5°C. The temperature histories were determined from the program CrackTeSt COIN, using the obtained hydration heat development for each concrete and the geometry of the wall as input.

4. EAC Design Methodology

The current EAC design methodology is pragmatic in the way that it includes high activity in the laboratory. The focus has been on making the method accurate and advanced, but still practical and easy applicable for contractors and structural designers. The basis of the methodology is to define and describe a given concrete through laboratory testing and succeeding model fitting. The obtained material parameters are then evaluated and calibrated by comparing (1) stress development measured in a Temperature-Stress Testing Machine with (2) stress development calculated by various EAC calculation approaches using the obtained material properties. The main steps in the EAC design methodology are illustrated in Figure 3 and described as follows:

(a) Material properties, such as heat, strength, and E-modulus development over time, are determined from dedicated laboratory tests for the investigated concrete

(b) Selected material models are fitted to the test results to provide numerical descriptions of the various properties

(c) A material database is established, comprising material properties and corresponding model parameters for the given concrete

(d) A restrained stress test is performed in the TSTM, where the specimens are subjected to a curing temperature regime representing a selected section of an 800 mm thick wall structure

(e) The TSTM stress development is "back-calculated" by various EAC calculation approaches based on the established material database

(f) The material database is evaluated and calibrated by comparing the calculated stress development with the stress development measured in the TSTM

The above-described steps result in a material database that can be used for early age crack assessment and structural design for a given concrete. The tests in the TSTM constitute a valuable calibration and verification of the established material database. In addition, the TSTM tests include the

Table 2: Test programme.

Concrete	Test	No. of specimens	Test age (days)
ANL ref.	Heat development	1	0–5
	Direct tensile strength	2 + 2	2, 28
	Compressive cube strength	3 · 8	1, 1.5, 2, 3, 4, 5, 7, 28, 90
	TSTM (summer conditions)	3	—
ANL FA17	Heat development	1	0–5
	Direct tensile strength	2 + 2	2, 28
	Compressive cube strength	3 · 8	1, 1.5, 2, 3, 4, 5, 7, 28, 90
	TSTM (summer + winter)	2 + 1	—
ANL FA33	Heat development	1	0–5
	Direct tensile strength	2 + 2	2, 28, 91
	Compressive cube strength	3 · 8	1, 1.5, 2, 3, 4, 5, 7, 28, 90
	TSTM (summer)	1	—
ANL FA45	Heat development	1	0–5
	Direct tensile strength	2 + 2	3, 28, 91
	Compressive cube strength	3 · 8	1, 1.5, 2, 3, 4, 5, 7, 28, 91
	TSTM (summer + winter)	1 + 1	—

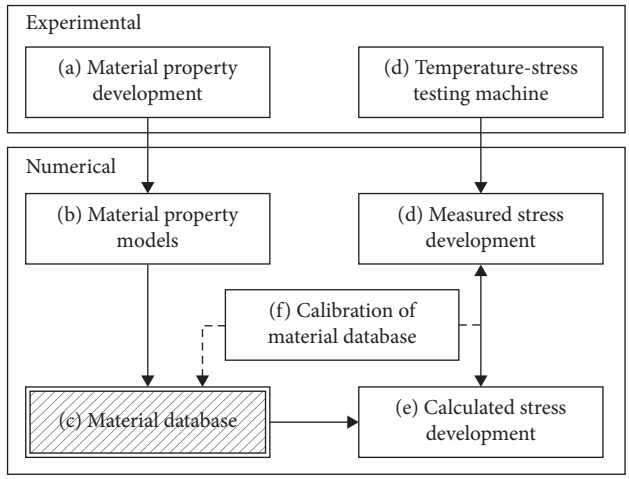

Figure 3: Flow chart of EAC design methodology.

effect of a realistic temperature curing regime on EAC and the corresponding material parameters.

5. Material Models and Early Age Stress Calculations

The current study applies the maturity principle, and the compressive strength, tensile strength, and E-modulus were modelled by equation (1), which is a modified version of the CEB-FIP MC 1990-model [50] (see [51–53]):

$$X(t_e) = X(28) \cdot \left\{ \exp\left[s \cdot \left(1 - \sqrt{\frac{672 - t_0}{t_e - t_0}} \right) \right] \right\}^n, \quad (1)$$

where $X(t_e)$ is the property as a function of maturity t_e, $X(28)$ is the property at 28 days, s and n are curve-fitting parameters, and t_0 is the start time for stress development (maturity time).

Consequently, the equations describing the compressive strength, tensile strength, and E-modulus are as presented in equation (2)–(4), respectively. The s parameter is the same for all properties, while the n parameter is varying [51, 52]:

$$f_c(t_e) = f_{c28} \cdot \left\{ \exp\left[s \cdot \left(1 - \sqrt{\frac{672 - t_0}{t_e - t_0}} \right) \right] \right\}^{n_c}, \quad n_c = 1, \quad (2)$$

$$f_t(t_e) = f_{t28} \cdot \left\{ \exp\left[s \cdot \left(1 - \sqrt{\frac{672 - t_0}{t_e - t_0}} \right) \right] \right\}^{n_t}, \quad (3)$$

$$E_c(t_e) = E_{c28} \cdot \left\{ \exp\left[s \cdot \left(1 - \sqrt{\frac{672 - t_0}{t_e - t_0}} \right) \right] \right\}^{n_E}. \quad (4)$$

In the above-described equations, the start time for stress development t_0 was found from the TSTM tests as the maturity time when the measured restrained stress reaches 0.1 MPa for tests performed under realistic (summer) temperature. The other model parameters were found by fitting the above-described models to the corresponding test results by using the method of least squares.

The uniaxial stress development in the TSTM was back-calculated, i.e., simulated, by three different calculation approaches: TSTM-sim, CrackTeSt COIN, and DIANA. TSTM-sim serves as a specially designed low-threshold method to back-calculate the stress development measured in the TSTM in order to calibrate and/or verify the material parameters and models used. The alternative calculation methods CrackTeSt COIN and DIANA were included in order to evaluate and verify the TSTM-sim approach. Simultaneously, TSTM-sim in combination with restrained stress tests in the TSTM constitutes an evaluation of DIANA and CrackTeSt COIN for practical purposes.

TSTM-sim is a specially designed 1D calculation routine programmed in Excel and Visual Basic. The program

simulates the stress development in the TSTM using the following input parameters: (1) material parameters describing the given concrete, (2) temperature measured in the TSTM, (3) free deformation and temperature measured in the parallel dilation rig, and (4) the degree of restraint applied in the TSTM test. TSTM-sim applies the maturity principle and calculates E-modulus and tensile strength development over time. Subsequently, the creep and stress development over time are computed. The time-dependent stress response of concrete is described based on linear viscoelasticity for ageing materials, which implies that the creep strains under a constant stress are linearly related to the stress level. This linearity was modelled by the compliance function $J(t,t')$ combined with the Double Power Law [54]:

$$J(t,t') = \frac{1}{E_c(t'_e)}\left[1 + \varphi_0 \cdot t_e'^{-d} \cdot (t-t')^p\right], \quad (5)$$

where t (days) is the concrete age, t' is the concrete age at which the actual stress was applied, $E_c(t'_e)$ is the E-modulus at t'_e, t'_e is the equivalent age (maturity) at t', and φ_0, d, and p are creep model parameters.

The principle of superposition applied ageing of concrete can be interpreted as "*... the strains produced at any time t by a stress increment applied at age $t' < t$ are independent of the effects of any stress applied earlier or later*" [9]. By combining the theory of linear viscoelasticity with the principle of superposition, the total strain for a variable stress history can be expressed in discrete form by equation (6), which is the basis for the TSTM back-calculations in TSTM-sim [15]:

$$\varepsilon(t) = \sum_0^t J(t,t') \cdot \sigma(t') + \varepsilon_{as}(t) + \varepsilon_T(t), \quad (6)$$

where the total strain increment generated over a time interval $(\Delta\varepsilon = \varepsilon(t_2) - \varepsilon(t_1))$ is given by the actual degree of restraint in the TSTM, $J(t,t')$ is the compliance function, $\Delta(\sigma(t'))$ is a stress increment induced at time t', and $(\varepsilon_{as}(t) + \varepsilon_T(t))$ is the free deformation measured in the dilation rig.

The creep model used in TSTM-sim is not unique, and several alternative approaches are found in the literature (e.g., [55–57]). The currently used model constitutes a simplification of the real material performance, and it was chosen based on previous experience at NTNU, where it has been found to be suitable and sufficiently accurate when evaluating creep test results and performing EAC calculations.

The 2D special-purpose program CrackTeSt COIN [58] was also used to simulate the stress development in the TSTM during testing. CrackTeSt COIN calculates temperature, strength, stress, and cracking risk over time in hardening concrete structures. An early age stress calculation in CrackTeSt COIN consists of a heat flow analysis followed by a structural analysis. The time-dependent stress response is described by a Maxwell chain model, i.e., the calculations are based on relaxation curves. The creep parameters were therefore converted to relaxation data by the program RELAX [59] prior to the TSTM simulations in CrackTeSt COIN. In the TSTM back-calculations, the concrete temperature development was modelled as an external temperature history over time. The free dilation measured in the dilation rig was applied the TSTM model as follows: (1) thermal dilation induced by the enforced temperature development and (2) autogenous deformation applied as concrete shrinkage.

DIANA [60], a well-known multipurpose 3D FEM program, was the third approach used to simulate the stress development in the TSTM. In DIANA, the TSTM simulation was performed as a staggered flow-stress analysis. This involves a transient heat flow analysis followed by a structural analysis. Also for the DIANA analyses, the temperature development in the modelled concrete specimen was applied as an external temperature history over time. The measured free dilation in the dilation rig was applied to the TSTM model as a time dependent prescribed displacement; hence, the thermal expansion and the shrinkage strains in the material model were set to zero since they were already taken into account by the dilation rig measurements. In DIANA, both the Double Power Law and Maxwell chains are available when describing the creep/relaxation behaviour of the concrete. As opposed to the previously described Excel calculation, the creep ratio, $\phi(t,t')$, in DIANA is not maturity dependent. For the calculations based on relaxation and Maxwell chains, the given creep parameters were transformed to relaxation data by the program RELAX [59].

The currently used approaches for early age stress calculations are more thoroughly described in [15].

6. Results and Discussion

Test results and deduced model parameters for the investigated concretes are presented in Table 3 and Figure 4. The activation energy parameters A and B in Table 3 were determined based on compressive strength tests on specimens cured under 5°C, 20°C, and 35°C, respectively. These tests and the succeeding derivations are described and reported in detail in [15].

The semiadiabatic calorimeter test results confirmed the well-known fact that the concrete heat evolvement is systematically decreasing with increasing amount of fly ash (Figure 4(a)). It should, however, be noticed that the currently used ANL FA cement had quite an aggressive hydration heat evolvement when compared to previously used batches of ANL FA cement. In fact, the hydration heat evolvement of the currently used ANL FA (16.6% fly ash) was almost as high as that of ANL ref. (without fly ash). This irregular high hydration heat evolvement could be caused by an unfavorable combination of a rather high fineness (Blaine: 389 m^2/kg) and a slightly lower fly ash content (16.6%) when compared to a previous tested batch that had a fineness and a fly ash content of 370 m^2/kg and 17.8%, respectively. The hydration heat evolvement for a given batch of cement is also influenced by other parameters, such as cement composition and fly ash batch. These results illustrate that the heat evolvement in the hardening phase can vary considerably between different batches of cement, and

Table 3: Deduced material model parameters.

	A	B	t_0	s	n_t	n_E	f_{c28} (MPa)	f_{t28} (MPa)	E_{28} (GPa)	E_{TSTM} (GPa)	CTE	ϕ_0	d	p
ANL ref.	31500	300	8.8	0.200	0.484	0.348	80.3	3.9	32.5	32.8	9.0	0.75	0.20	0.21
ANL FA17	31500	200	9.5	0.275	0.589	0.299	71.2	3.6	30.6	31.5	9.1	0.67	0.32	0.28
ANL FA33	37000	0	12.0	0.356	0.486	0.252	53.6	3.1	27.8	30.5	9.2	0.49	0.22	0.33
ANL FA45	42000	0	13.0	0.424	0.665	0.189	45.3	3.0	24.9	29.5	9.4	0.30	0.24	0.35

it underlines the importance of regular heat evolution tests during the construction period.

The 28-day compressive strength, which is the most commonly used quality class parameter, was systematically decreasing with increasing fly ash content. However, due to the considerable property increase beyond 28 days was seen for the fly ash concretes, the difference in compressive strength between the investigated concretes seemed to be decreasing over time. At 91 days, the compressive strength of ANL ref. and ANL FA were in the same range (Figure 4(c)). The deduced s parameters, which describe the compressive strength development of the concretes, are given in Table 3. The s values were in the same order of magnitude as found in other studies (e.g., [51, 61]).

The 28-day tensile strength was also decreasing with increasing amount of fly ash (Figure 4(d)). However, the differences in tensile strength between the concretes were decreasing over time due to the considerable late property development seen for fly ash concretes. The models actually indicate that the tensile strength of ANL FA45 surpasses ANL FA33 at approximately 28 days. The model parameters were found from mechanical testing up until 28 days according to common practice. Hence, the model and its parameters do not accurately describe the considerable property development beyond 28 days for the fly ash concretes. While the model predicts a tensile strength of 3.3 MPa and 3.4 MPa at 91 days for ANL FA33 and ANLFA45, respectively, the actual measured tensile strength was much higher: 4.1 and 4.0 MPa, respectively. This should be taken into account when evaluating the tensile strength and risk of cracking beyond 28 days, but for most structures, the main risk of EAC will occur prior to 28 days. Further research and more data are required to achieve reliable models that include the late property development of fly ash concretes.

The tensile E-modulus was found to decrease with increasing fly ash content for all test ages (Figure 4(e)). During the current study, unsatisfying agreement was seen between the E-modulus found from the test program, E_{28}, and the E-modulus deduced from stress-strain increments in the TSTM, E_{TSTM}. It was suspected that realistic temperature curing conditions could have an effect on the mechanical properties. Therefore, a series of mechanical testing was carried out with the aim to investigate the effect of curing temperature on compressive strength, tensile strength, and E-modulus [16]. The test program showed that a realistic curing temperature regime caused an increase in the initial E-modulus development for the fly ash concretes that could not be accounted for by the maturity principle. It was therefore decided to increase the 28-day E-modulus according to the TSTM tests in the currently established material database (see Table 3).

The coefficient of thermal dilation (CTE) is a complex parameter that varies with both concrete mix constituents and time (degree of self-desiccation) [62]. The current work applied the commonly used simplification of a constant CTE, which was determined as an average value found from temperature loops at the end of restrained stress tests in the TSTM. A tendency of a slight increase in CTE with increasing amount of fly ash was seen in Table 3.

For each TSTM test, the AD development was deduced by removing TD from the total deformation measured in the dilation rig using the CTE. The AD developments for the investigated concretes are presented in Figure 4(f), where the graphs are zeroed at the starting time for stress development, t_0. It should be noticed that the AD curves are presented as a function of time and not maturity, i.e., they represent the AD development over time in the currently defined 800 mm thick wall for a given concrete exposed to its own individual curing temperature history. A considerable variation was seen in the deduced AD, which was found to be strongly dependent on the temperature increase during curing (see [15, 63]). The applied simplification of a constant CTE will introduce an inaccuracy to the deduced AD; however, the current stress calculations are based on the total measured deformation and are therefore not affected by the choice of CTE. If using the deduced AD in combination with another temperature history, the simplification of a constant CTE would only have a limited influence on the stress development, as the small possible inaccuracy of the AD occurs in a phase where the E-modulus is still rather low [15, 63].

The creep parameters originally used in the calculations were assumed based on previous experience with similar concretes. However, the TSTM back-calculations revealed a deviation between calculated and measured stress development that was increasing systematically with the fly ash content. This deviation was suspected to be caused by the assumed creep parameters and it was therefore decided to perform dedicated creep tests on ANL FA and ANL FA33 in the TSTM. These creep tests and the appurtenant results are described and presented by Klausen et al. [46]. The new model parameters provided much better agreement between measured and back-calculated stress development (Table 3 and Figure 5(a)). This exercise illustrates the main concept of the current TSTM methodology, using the TSTM as a "solution" in order to evaluate and calibrate the determined model parameters of the investigated concrete.

Figure 5(b) shows measured and calculated stress developments for ANL ref. subjected to a realistic temperature curing regime, representing Norwegian summer conditions. The stress developments were calculated by TSTM-sim, CrackTeSt COIN, and DIANA using the Double Power Law

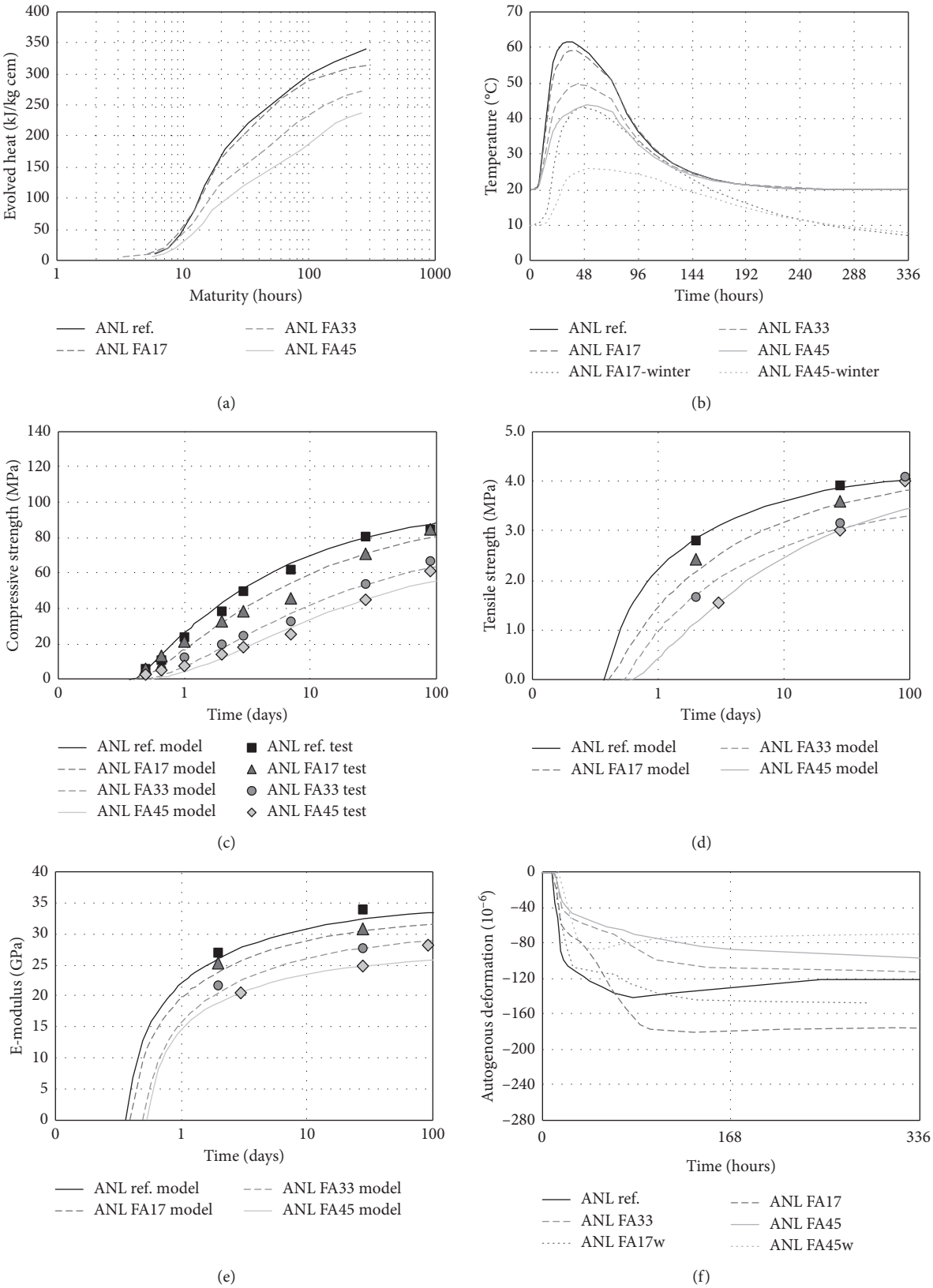

Figure 4: Heat and property development.

(DIANA DPL), and all approaches were based on the same material parameters. The calculated stress curves showed very good agreement, both with each other and also with the corresponding measured stress. All calculation approaches provided an accurate description of the compressive phase, while the DIANA calculation gave a slightly lower tensile stress development over time than the other approaches. The reason for this is situated in the creep calculations, as the creep ratio, $\phi(t, t')$, in DIANA is not maturity dependent. All in all, the calculation approaches combined with the previously determined material parameters must be said to provide a very accurate simulation of the stress development in the TSTM. A corresponding agreement between the various calculation approaches was also seen for the other investigated concretes, and consequently, the specially designed TSTM-sim simulation routine in Excel was evaluated and verified by CrackTeSt COIN and DIANA. In the following, TSTM-sim has been used to back-calculate the measured stress development in order to evaluate and verify the material properties for the rest of the concretes.

Measured and calculated stress developments for the investigated concretes subjected to realistic temperature curing regimes representing Norwegian summer conditions are presented in Figure 6. It should be noticed that each concrete was subjected to its own semiadiabatic temperature history, representing a section of an 800 mm thick wall (Figure 5(b)). To differentiate between the concretes and their individual temperature histories, the following notation was used: "*Concrete name* (T_{ini}/T_{max})," where T_{ini} is the initial temperature of the fresh concrete and T_{max} is the maximum concrete temperature during testing. All realistic temperature tests in the TSTM were applied a degree of restraint of $R = 50\%$.

Figure 6(a) shows measured and calculated stress development for three nominal identical TSTM tests performed with ANL ref. The measured stress development showed very good reproducibility between the tests, with a standard deviation at 48 and 96 hours of only 0.03 and 0.06 MPa, respectively. In addition, there was also a very good agreement between the measured stress development and the corresponding back-calculation. For ANL FA, two nominal identical TSTM tests were performed (Figure 6(b)). The tests provided very similar measured stress developments, as well as good agreement between measured and calculated stress. Figures 6(c) and 6(d) show measured and calculated stress developments for ANL FA33 and ANL FA45, respectively. Both tests showed rather good agreement between measured and calculated stress; however, a small underestimation of the tensile stress development over time was seen for ANL FA33. This small deviation could be caused by a temperature-induced initial increase in the E-modulus. Although the temperature effect on the 28-day value for the E-modulus was corrected for by replacing E_{28} with E_{TSTM}, a corresponding temperature-induced increase in the E-modulus development rate over the first few days has not been accounted for (see [15, 16]). In summary, the TSTM provided very good reproducibility for the nominal identical tests. In addition, the TSTM tests and the corresponding back-calculations verified the calculation approaches and the established material database for all investigated concretes.

The Norwegian climate with its cold winters can be challenging when it comes to concrete construction. It has been seen that the tensile strength for high-volume fly ash concretes can be very slow at low/moderate temperatures, and it was suspected that this effect could override the beneficial effect of reduced heat development. Therefore, it was decided to perform tests in the TSTM, where the concrete was subjected to Norwegian winter conditions, which in the current study was defined to involve a fresh concrete temperature of 10°C and an ambient temperature of 5°C. Figure 7 shows measured and calculated stress development for ANL FA17 and ANL FA45 exposed to winter conditions. Measured and back-calculated stress developments gave good agreement also for these temperature curing conditions. Hence, the current EAC methodology proves robust, as the established material database was found to be valid also for temperature curing conditions representing other climatic conditions.

Figure 8(a) shows a compiled set of stress development curves measured in the TSTM. When focusing on the fly ash concretes only (which all are based on the same cement Anlegg FA), both the compressive and tensile stresses were decreasing with increasing fly ash content for the given wall example and temperature conditions (800 mm thick wall, summer and winter conditions). As seen in Figure 4(a), the maximum temperature during curing, T_{max}, is decreasing with increasing fly ash content. Consequently, a reduction in T_{max} reduces both the concrete expansion, i.e., the initial compressive stress development, and the thermal contraction during the cooling phase. However, this fly ash-induced reduction in tensile stress development must be considered in combination with the corresponding reduced tensile strength. Therefore, the crack tendency of the concretes was evaluated based on the crack index, i.e., the occurring tensile stress divided by the corresponding tensile strength (see Figure 8(b)). For the investigated concretes and structural case, an increasing replacement of cement by fly ash was found to reduce the cracking tendency. The concrete with the highest fly ash content, ANL FA45, was found to provide the lowest crack index for both summer and winter conditions for the given 800 mm thick wall.

The ANL ref. tests contributed significantly in regards of reproducibility documentation of the TSTM; however, they were not directly comparable with the fly ash concretes as they were made from different cement. Originally, the ANL ref. concrete without fly ash was expected to give the highest cracking tendency. However, due to a combination of several unfavorable circumstances, the cracking risk of both ANL FA17 and ANL FA33 actually surpassed ANL ref. over time (Figure 8(b)). The reasons for this were (1) the irregular high hydration heat evolution of the currently used ANL FA cement batch, (2) the high AD seen for fly ash concretes exposed to high curing temperatures, (3) the temperature-induced increase in E-modulus at early ages observed for fly ash concretes, and (4) the low tensile strength development rate at early ages for fly ash concretes.

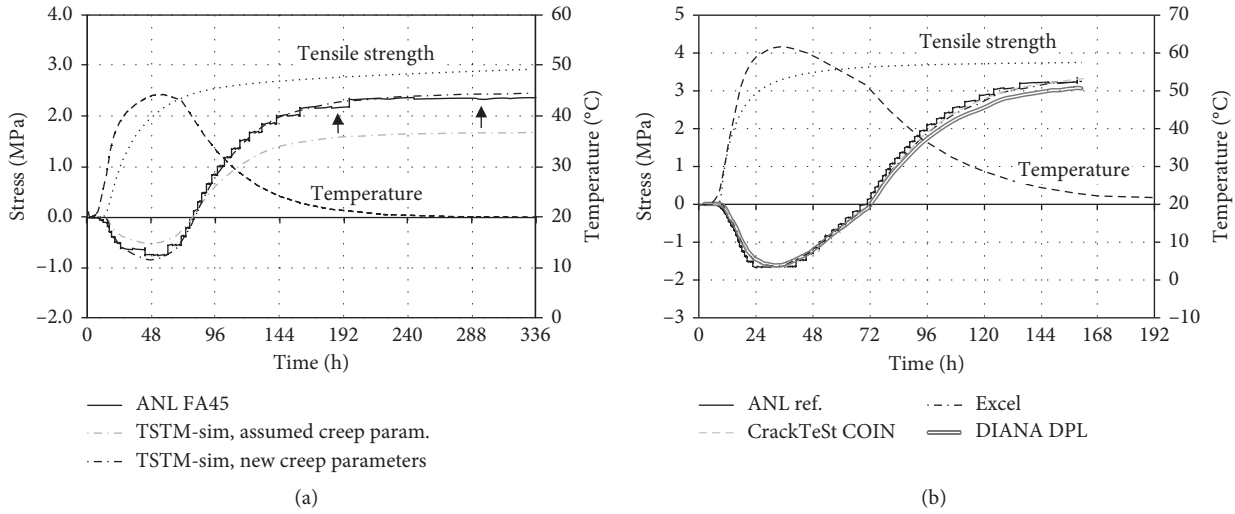

Figure 5: Measured and calculated stress development in the TSTM: ANL FA45 (a) and ANL ref. (b).

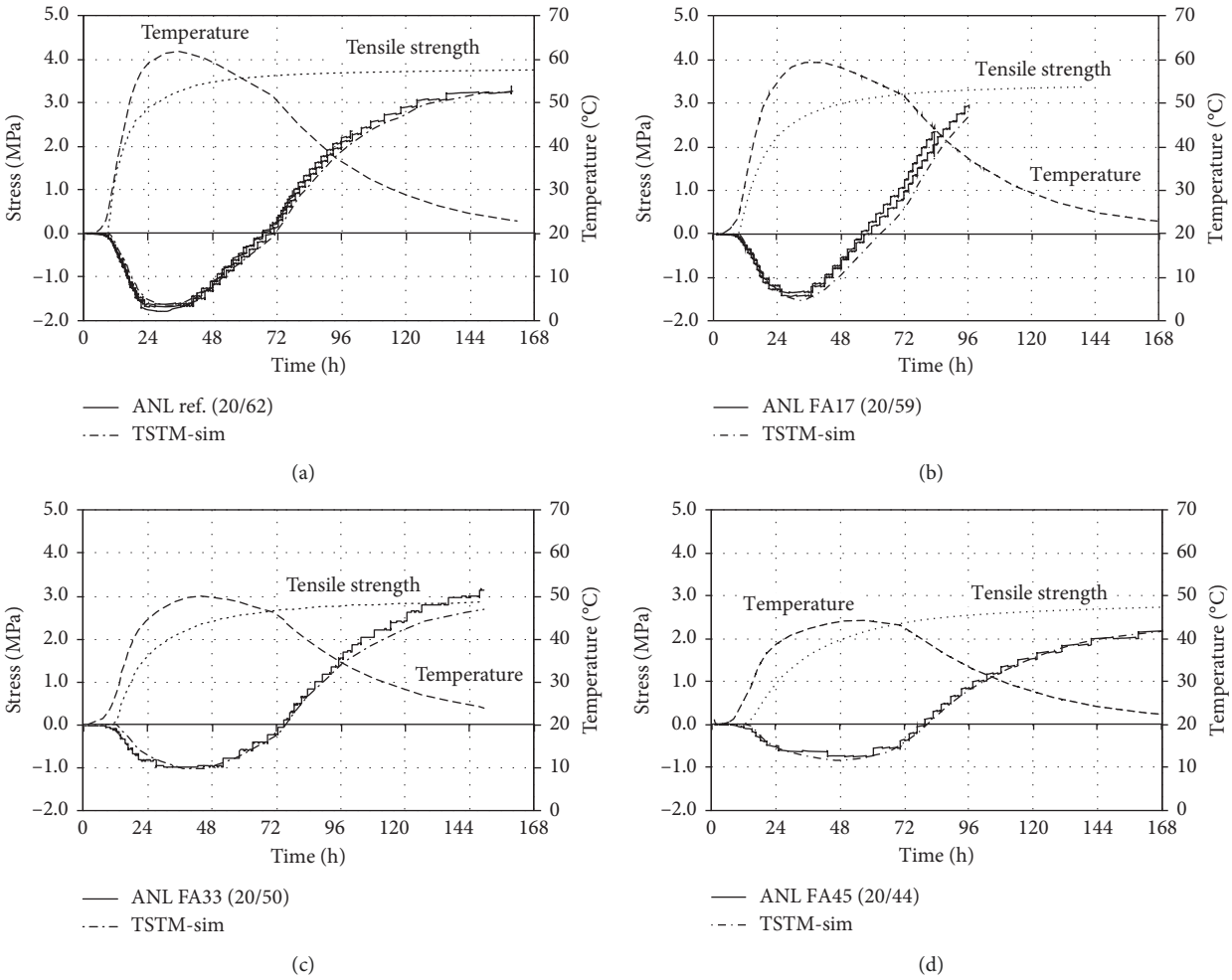

Figure 6: Measured and calculated stress development: ANL ref. (a), ANL FA17 (b), ANL FA33 (c), and ANL FA45 (d).

The current article shows that replacing cement with fly ash could reduce the cracking tendency of concrete; however, the risk of EAC is also influenced by several other parameters such as e.g., cement batch, aggregate type, w/c-ratio, and addition of shrinkage-reducing admixtures (SRA) [64]. Accurate concrete property characterization and

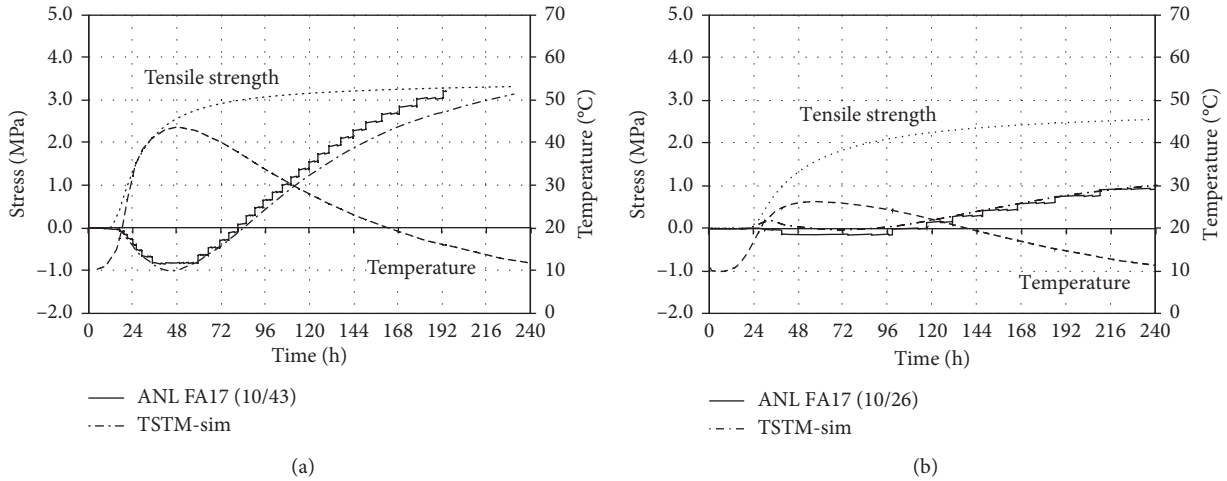

Figure 7: Stress development winter conditions: ANL FA17 (a) and ANL FA45 (b).

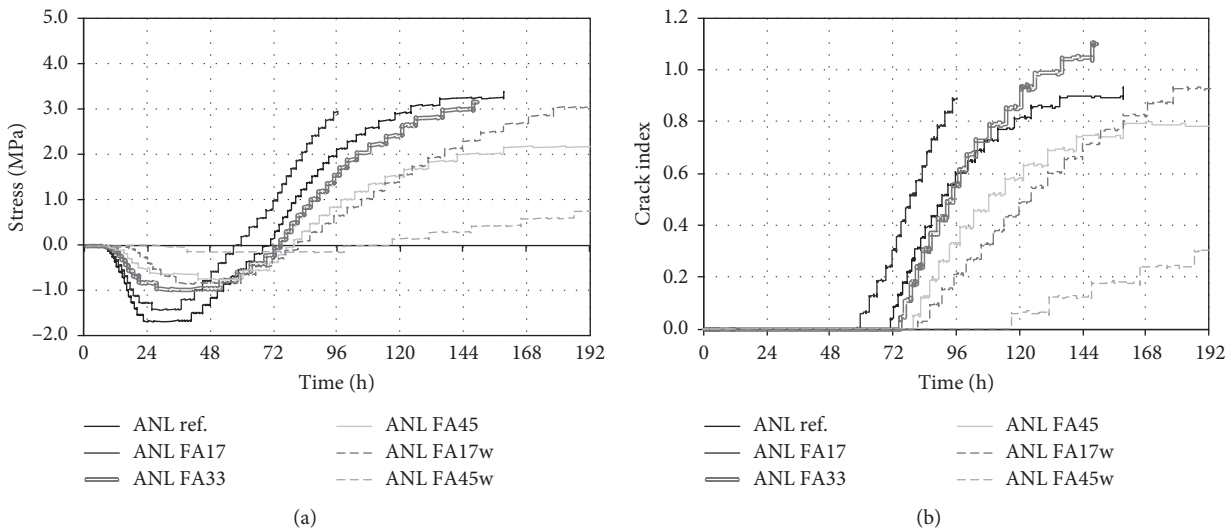

Figure 8: Measured stress development in the TSTM (a) and deduced crack index (b).

corresponding EAC design methodologies should therefore be included in design of concrete structures, where EAC could be an issue.

7. Summary and Conclusion

A design methodology on early age cracking (EAC) and a corresponding concrete property characterization method based on laboratory testing and the Temperature-Stress Testing Machine (TSTM) has been established and developed during the current work:

(i) The TSTM provided very good reproducibility and reliable results during the study. For instance, creep parameters directly deduced from restrained stress tests in the TSTM gave very good agreement with corresponding dedicated creep tests. Due to its reliability, tests in the TSTM constitute a valuable calibration and verification of the material and model parameters established for a given concrete. In addition, the TSTM tests include the effect of a realistic temperature curing regime on EAC and the corresponding material parameters.

(ii) Good agreement was found between early age stress developments calculated with TSTM-sim (Excel), CrackTeSt COIN, and DIANA, respectively. When correcting for the temperature effect on the 28-day value for the E-modulus, the calculations also showed very good agreement with the corresponding stress development measured in the TSTM, both for summer and winter temperature curing conditions. This overall agreement supports the validity and robustness of the calculation approaches as well as the applied model parameters.

(iii) Based on the current property mapping and calibration, a material database for the investigated concretes was established in the special-purpose program CrackTeSt COIN. CrackTeSt COIN and

the appurtenant material database now constitute a facility by which contractors and structural designers can estimate proper choice of concrete type, mineral additives, and execution methods on-site to minimize or even avoid cracking.

(iv) Several material parameters that affect EAC are dependent on the concrete curing temperature in a way that only to a certain extent can be described by the maturity principle, e.g., tensile strength, E-modulus, and autogenous deformation (AD). Hence, the current results strongly suggest that such parameters should be measured under relevant realistic temperature curing conditions.

(v) For the investigated concretes and structural case, an increasing replacement of cement by fly ash was found to reduce the cracking tendency.

In the years to come, concrete is expected to change due to its current contribution to CO_2 emissions and its use of natural resources. The industry needs to be prepared for property characterization and EAC design of the upcoming next generation of concretes with low-CO_2 cements and recycled aggregate.

Data Availability

The data used to support the findings of this study are available from the corresponding author upon request.

Disclosure

The current publication is based on the Ph.D. thesis "Early age crack assessment of concrete structures, experimental determination of decisive parameters" by Klausen [15].

Conflicts of Interest

The authors declare that they have no conflicts of interest.

Acknowledgments

The work has been performed within the User-driven Research-based Innovation project DaCS (Durable advanced Concrete Solutions, 2015–2019) at COIN (Concrete Innovation Centre, 2007–2014 (https://www.sintef.no/en/projects/coin/coinp), a Centre for Research-based Innovation established by the Research Council of Norway).

References

[1] Norsk Standard, *NS-EN 1992-1-1:2004+NA:2008, Eurocode 2: Design of Concrete Structures, Part 1-1: General Rules and Rules for Buildings*, Norsk Standard, Oslo, Norway, 2004.

[2] CIRIA, *C766—Control of Cracking Caused by Restrained Deformation in Concrete*, CIRIA, London, UK, 2018.

[3] FIB, *Model Code for Concrete Structures*, FIB, Berlin, Germany, 2010.

[4] Research Project CEOS.fr, *Control of Cracking in Reinforced Concrete Structures*, Wiley, Hoboken, NJ, USA, 2016.

[5] Norsk Standard, *NS 3473:2003-Prosjektering Av Betongkonstruksjoner, Beregnings-Og Konstruksjonsregler*, Norsk Standard, Oslo, Norway, 2003.

[6] Japan Concrete Institute (JCI), *JCI Guidelines for Control of Cracking of Mass Concrete*, Japan Concrete Institute (JCI), Tokyo, Japan, 2008.

[7] Bundesanstalt für Wasserbau (BAW), *Rissbreitenbegrenzung für frühen Zwang in Massiven Wasserbauwerken (MFZ)*, Bundesanstalt für Wasserbau (BAW), Karlsruhe, Germany, 2011.

[8] CEN/TC 104, *DRAFT: prEN 12390-16 Testing Hardened Concrete—Part 16: Determination of the Shrinkage of Concrete*, CEN, Brussels, Belgium, 2018.

[9] A. M. Neville, *Properties of Concrete*, Pearson, London, UK, 5th edition, 2011.

[10] J. Lindgård and E. J. Sellevold, "Is high strength concrete more robust against elevated temperatures?" in *Proceedings of Third International conference on Utilization of High Strength Concrete*, I. Holand and E. J. Sellevold, Eds., pp. 810–821, Lillehammer, Norway, June 1993.

[11] Ø. Bjøntegaard and E. J. Sellevold, "Thermal dilation-autogenous shrinkage: how to separate?" in *International Workshop on Autogenous Shrinkage of Concrete*, E.-I. Tazawa, Ed., pp. 245–256, JCI, Hiroshima, Japan, 1998.

[12] Ø. Bjøntegaard, *Thermal dilation and autogenous deformation as driving forces to self-induced stresses in high performance concrete*, Ph.D. thesis, Norwegian University of Science and Technology (NTNU), Trondheim, Norway, 1999.

[13] O. M. Jensen and P. F. Hansen, "Influence of temperature on autogenous deformation and relative humidity change in hardening cement paste," *Cement and Concrete Research*, vol. 29, no. 4, pp. 567–575, 1999.

[14] T. Kanstad, T. A. Hammer, Ø. Bjøntegaard, and E. J. Sellevold, "Mechanical properties of young concrete—part I: experimental results related to test methods and temperature effects," *Materials and Structures*, vol. 36, no. 258, pp. 218–225, 2003.

[15] A. E. Klausen, *Early age crack assessment of concrete structures, experimental determination of decisive parameters*, Ph.D. thesis, Norwegian University of Science and Technology (NTNU), Trondheim, Norway, 2016, https://ntnuopen.ntnu.no/ntnu-xmlui/handle/11250/2430293.

[16] A. E. Klausen, T. Kanstad, Ø. Bjøntegaard, and E. J. Sellevold, "The effect of realistic curing temperature on the strength and E-modulus of concrete," *Materials and Structures*, vol. 51, no. 6, p. 168, 2018.

[17] R. Springenschmid, "Prevention of thermal cracking in concrete at early ages—preface," RILEM Report 15, RILEM, Paris, France, 1998.

[18] R. Springenschmid, R. Breitenbücher, and M. Mangold, "Development of the cracking frame and the temperature-stress testing machine," in *Proceedings of the International Symposium held by RILEM: Thermal Cracking in Concrete at Early Ages*, Munich, Germany, October 1994.

[19] H. Hedlund, *Hardening concrete, measurements and evaluation of non-elastic deformation and associated restraint stresses*, Ph.D. thesis, Luleå University of Technology, Luleå, Sweden, 2000.

[20] F. Czerny, K. van Breugel, and E. A. B. Koenders, "The reliability of crack predictions for hardening concrete structures," in *Proceedings of the International Congress—Global Construction: Ultimate Concrete Opportunities*, Dundee, Scotland, July 2005.

[21] M. N. Amin, J.-S. Kim, Y. Lee, and J.-K. Kim, "Simulation of the thermal stress in mass concrete using a thermal stress

measuring device," *Cement and Concrete Research*, vol. 39, no. 3, p. 11, 2009.

[22] A. Darquennes, S. Staquet, M.-P. Delplancke-Ogletree, and B. Espion, "Effect of autogenous deformation on the cracking risk of slag cement concretes," *Cement and Concrete Composites*, vol. 33, no. 3, pp. 368–379, 2011.

[23] D. Shen, J. Jiang, J. Shen, P. Yao, and G. Jiang, "Influence of curing temperature on autogenous shrinkage and cracking resistance of high-performance concrete at an early age," *Construction and Building Materials*, vol. 103, pp. 67–76, 2016.

[24] J. Xin, G. Zhang, Y. Liu, Z. Wang, and Z. Wu, "Effect of temperature history and restraint degree on cracking behavior of early-age concrete," *Construction and Building Materials*, vol. 192, pp. 381–390, 2018.

[25] D. H. Nguyen, V. T. Nguyen, P. Lura, and V. T. N. Dao, "Temperature-stress testing machine—a state-of-the-art design and its unique applications in concrete research," *Cement and Concrete Composites*, vol. 102, pp. 28–38, 2019.

[26] A. E. Klausen, T. Kanstad, and Ø. Bjøntegaard, "Updated temperature-stress testing machine (tstm): introductory tests, calculations, verification and investigation of variable fly ash content," in *Proceedings of CONCREEP 10*, Vienna, Switzerland, September 2015.

[27] RILEM Technical Committee 119, *Proceedings of the International RILEM Symposium: Thermal Cracking in Concrete at Early Ages*, R. Springenschmid, Ed., Technical University of Munich, Munich, Germany, 1994.

[28] Japan Concrete Institute (JCI), *Autogenous Shrinkage of Concrete: Proceedings of the International Workshop Organised by JCI (Japan Concrete Institute), Hiroshima, June 13-14, 1998*, E.-I. Tazawa and N. K. K. Kyokai, Eds., E & FN Spon, New York, NY, USA, 1998.

[29] RILEM Technical Committee 119, *State-of-The-Art Report: Prevention of Thermal Cracking in Concrete at Early Ages*, R. Springenschmid, Ed., Technical University of Munich, Munich, Germany, 1998.

[30] RILEM, *International RILEM Workshop on Shrinkage of Concrete (Shrinkage 2000)*, V. Baroghel-Bouny and P.-C. Aïtcin, Eds., RILEM Publications, Paris, France, 2000.

[31] K. Kovler and A. Bentur, "International RILEM conference on early age cracking in cementitious systems (EAC'01), Haifa, Israel, March 2001," *Materials and Structures*, vol. 34, no. 241, p. 446, 2001.

[32] A. Bentur, "Early age cracking in cementitious systems," in *Early Age Cracking in Cementitious Systems—Report of RILEM Technical Committee 181-EAS—Early Age Shrinkage Induced Stresses and Cracking in Cementitious Systems*, RILEM Publications, Paris, France, 2003.

[33] RILEM, *International RILEM Conference on Volume Changes of Hardening Concrete: Testing and Mitigation 20-23August 2006, Technical University of Denmark, Lyngby, Denmark*, O. M. Jensen, P. Lura, and K. Kovler, Eds., RILEM Publications, Paris, France, 2006.

[34] C. Hellmich, B. Pichler, and J. Kollegger, *CONCREEP 10, Proceedings of the 10th International Conference on Mechanics and Physics of Creep, Shrinkage and Durability of Concrete and Concrete Structures*, Vienna University of Technology, Vienna, Austria, 2015.

[35] D. Bosnjak, *Self-induced cracking problems in hardening concrete structures*, Ph.D. thesis, Norwegian University of Science and Technology (NTNU), Trondheim, Norway, 2000.

[36] P. F. Takacs, *Deformations in concrete cantilever bridges: observations and theoretical modelling*, Ph.D. thesis, Norwegian University of Science and Technology (NTNU), Trondheim, Norway, 2002.

[37] D. S. Atrushi, *Tensile and compressive creep of early age concrete: testing and modelling*, Ph.D. thesis, Norwegian University of Science and Technology (NTNU), Trondheim, Norway, 2003.

[38] G. Ji, *Cracking risk of concrete structures in the hardening phase*, Ph.D. thesis, Norwegian University of Science and Technology (NTNU), Trondheim, Norway, 2008.

[39] The Norwegian Public Roads Administration, *Handbook R762E: General Specifications 2: Standard Specification Texts for Bridges and Quays: Principal specification 8*, The Norwegian Public Roads Administration, Oslo, Norway, 2009.

[40] COIN, *Concrete Innovation Centre—A Centre for Research Based Innovation*, Research Counsil of Norway, Oslo, Norway, 2007, https://www.sintef.no/en/projects/coin/coinp.

[41] DACS, *Durable Advanced Concrete Solutions—A User-Driven Research-Based Innovation Project*, Research Counsil of Norway, Oslo, Norway, 2019, https://www.sintef.no/projectweb/dacs/.

[42] K. L. Scrivener, V. M. John, and E. M. Gartner, "Eco-efficient cements: potential economically viable solutions for a low-CO_2 cement-based materials industry," *Cement and Concrete Research*, vol. 114, pp. 2–26, 2018.

[43] NS 3657, *Concrete Testing—Determination of Heat Release*, Standards Norway, Oslo, Norway, 1993.

[44] INSTRON, *INSTRON 5985 250 kN*, INSTRON, Norwood, MA, USA, 2019, https://instron.us/-/media/literature-library/products/2013/02/5980-series-dual-column-floor-model-100kn--600kn.pdf.

[45] E. A. Hansen, *Time dependent tensile fracture of concrete*, Ph.D. thesis, Norwegian University of Science and Technology (NTNU), Trondheim, Norway, 1991.

[46] A. E. Klausen, T. Kanstad, Ø. Bjøntegaard, and E. Sellevold, "Comparison of tensile and compressive creep of fly ash concretes in the hardening phase," *Cement and Concrete Research*, vol. 95, pp. 188–194, 2017.

[47] T. Kanstad, D. Bosnjak, and J. A. Øverli, "3D restraint analyses of typical structures with early age cracking problems," IPACS Report, Luleå University of Technology, Luleå, Sweden, 2001.

[48] Ø. Bjøntegaard and E. J. Sellevold, "The temperature-stress testing machine (TSTM): capabilities and limitations," in *Proceedings of the Advances in Concrete Through Science and Engineering*, Evanston, IL, USA, March 2004.

[49] NS-EN 197-1, *Cement—Part 1: Composition, Specifications and Conformity Criteria for Common Cements*, Standards Norway, oslo, Norway, 2011.

[50] FIB, *CEB-FIP Model Code 1990: Design Code*, Comité Euro-International du Béton, Lausanne, Switzerland, 1991.

[51] T. Kanstad, T. A. Hammer, Ø. Bjøntegaard, and E. J. Sellevold, "Mechanical properties of young concrete—part II: determination of model parameters and test program proposals," *Materials and Structures*, vol. 36, no. 4, pp. 226–230, 2003.

[52] J.-E. Jonasson, P. Fjellström, and H. Bäckström, *Inverkan Av Variabel Härdningstemperatur På Betongens Hållfasthetsutveckling (The Influence of Variable Curing Temperature on the Strength Development of Concrete—Only Available in Swedish)*, Bygg & Teknik, Stockholm, Sweden, 2010.

[53] Ø. Bjøntegaard, "Basis for and practical approaches to stress calculations and crack risk estimation in hardening concrete structures—state of the art," COIN Project Report 31, SINTEF Building and Infrastructure, Trondheim, Norway, 2011.

[54] Z. P. Bazant and E. Osman, "Double power law for basic creep of concrete," *Materials and Structures*, vol. 9, no. 1, pp. 3–11, 1976.
[55] A.-W. Gutsch, "Viscoelastic behaviour of early age concrete," IPACS Report, Luleå University of Technology, Luleå, Sweden, 2001.
[56] Z. P. Bazant, "Prediction of concrete creep and shrinkage: past, present and future," *Nuclear Engineering and Design*, vol. 203, no. 1, pp. 27–38, 2001.
[57] G. De Schutter, "Fundamental study of early age concrete behaviour as a basis for durable concrete structures," *Materials and Structures*, vol. 35, no. 1, pp. 15–21, 2002.
[58] JEJMS Concrete AB, *CrackTeSt COIN*, JEJMS Concrete AB, Luleå, Sweden, 2012.
[59] J.-E. Jonasson and G. Westman, "RELAX—conversion of creep data to relaxation data by the program RELAX," IPACS Report, TU Luleå, Luleå, Sweden, 2001.
[60] TNO DIANA BV, *DIANA FEA*, TNO DIANA BV, Delft, Netherlands, 2010.
[61] A. Vollpracht, M. Soutsos, and F. Kanavaris, "Strength development of GGBS and fly ash concretes and applicability of fib model code's maturity function—a critical review," *Construction and Building Materials*, vol. 162, pp. 830–846, 2018.
[62] E. J. Sellevold and Ø. Bjøntegaard, "Coefficient of thermal expansion of cement paste and concrete: mechanisms of moisture interaction," *Materials and Structures*, vol. 39, no. 9, pp. 809–815, 2006.
[63] A. E. Klausen, T. Kanstad, Ø. Bjøntegaard, and E. J. Sellevold, "The effect of curing temperature on autogenous deformation of fly ash concretes," *Cement and Concrete Composites*, 2019.
[64] A. E. Klausen and T. Kanstad, *The Effect of Shrinkage Reducing Admixtures on Drying Shrinkage, Autogenous Deformation and Early Age Stress Development of Concrete*, In press.